EXPERIMENTAL STUDY OF PROTON BEAM HALO IN MISMATCHED BEAMS*

C. K. Allen, K. C. D. Chan, P. L. Colestock, R. W. Garnett, J. D. Gilpatrick, W. P. Lysenko, J. D. Schneider, R. L. Sheffield, H. V. Smith, and T. P. Wangler,
Los Alamos National Laboratory, Los Alamos, NM 87545, USA

J. Qiang, Lawrence Berkeley National Laboratory, Berkeley, CA, USA

K. R. Crandall, TechSource, Santa Fe, NM, USA

M. E. Schulze, General Atomics, Los Alamos, NM, USA

Abstract

We report measurements of transverse beam-halo formation in mismatched proton beams in a 52-quadrupole FODO-transport channel following the 6.7 MeV RFQ at the Low-Energy Demonstration Accelerator (LEDA) at Los Alamos. Beam profiles in both transverse planes were measured using a new diagnostic device that consists of a movable carbon filament for measurement of the beam core, and scraper plates for measurement of the outer part of the distributions. The initial results indicate a surprisingly strong growth rate of the rms emittance even for the modest space-charge tune depressions of the experiment. Our results are consistent with the complete transfer of free energy of the mismatched beams into emittance growth within 10 envelope oscillations for both the breathing and the quadrupole modes.

1 INTRODUCTION

Theoretical research during the past decade has led to a picture of space-charge forces in mismatched beams as a major source of beam halo in high-current proton beams. The nonlinear space-charge force experienced by individual particles, while the beam is undergoing coherent rms-size oscillations, slowly drives some particles to larger amplitudes to form a halo. The mechanism has been described by a particle-core model [1, 2, 3] and identified as a parametric resonance [2]. An experiment has been carried out at Los Alamos to test these ideas.

2 THE EXPERIMENT

A 52-quadrupole FODO beam-transport channel was installed at the end of the Low-Energy Demonstration Accelerator (LEDA) 6.7-MeV, CW, 350-MHz RFQ to carry out an experimental study of beam-halo formation in a proton beam [4,5,6]. The channel allows the development of about 10 mismatch oscillations, enough to observe emittance growth and halo formation caused by mismatch. A large complement of beam diagnostics was provided [7]. The key diagnostic component was a unique transverse beam profile scanner [8] consisting of a thin, 33-μm diameter, carbon wire for measurement of the dense beam core, and mounted on a common movable frame, a pair of 1.5-mm thick scraper plates which increased the dynamic range for measurement of the halo. As the protons passed through the wire a signal was induced from secondary electron emission. The scraper plates were water cooled and were constructed of graphite brazed onto copper. An electrical signal was induced by the beam protons that stopped in the plates.

The data from the wires and the plates were combined using computer software to produce a single distribution with a dynamic intensity range of about 10^5:1. Nine measurement stations, shown in Fig. 1, were located midway between pairs of quadrupoles; both the horizontal and vertical projected distributions were measured at each location. The first station was located after quadrupole 4. The next stations were located after the beam had debunched after quadrupoles 20, 22, 24, 26, 45, 47, 49, and 51, as shown in the figure.

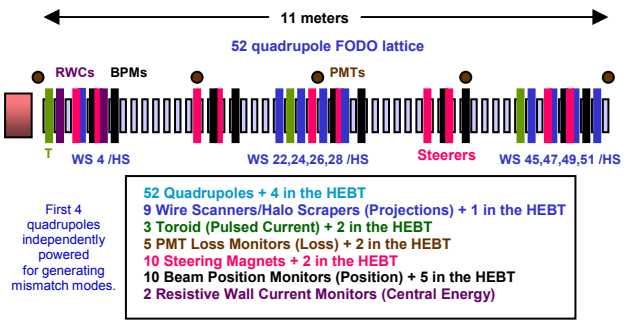

Figure 1: Block diagram of the 52 quadrupole transport channel showing the locations of the 9 profile scanners.

Beam matching was done by adjusting the first four quadrupoles to produce equal rms sizes in both x and y at wire scanner locations 22-28 and 45-51. The estimated error in the measurement of the rms beam sizes was ±50μm, limited primarily by transverse beam jitter. A least-squares-fitting procedure based on measurements of derivatives of rms sizes with respect to the four matching quadrupole gradients was used to match the beam. The

* Work sponsored by the US Dept. of Energy

Courant-Snyder parameters of the matched beam can be calculated from beam dynamics simulations using the measured values of the matched rms beam sizes. Pure mode mismatches were calculated by scaling the Courant-Snyder parameters to the desired values and finding the settings of the matching quadrupoles that produced these values. For example, multiplying each of the four transverse Courant-Snyder parameters α_x, β_x, α_y, and β_y by the same scaling factor produced a pure breathing-mode mismatch. The mismatch strength was measured by a parameter μ, which equals the ratio of the rms size of the initial mismatched beam to that of the matched beam.

The beam from the ion source was pulsed at 1 Hz to avoid damaging the interceptive beam diagnostics. The measurement cycle consisted of the following steps: The CW RFQ was de-energized with an RF blanking pulse, as the ion source was turned on. While the 75-keV injector beam current increased (approximately 1.5-ms rise time), the beam was injected into the un-powered RFQ. After about 2 msec, the RF blanking pulse was removed; the RFQ fields approached a steady state after another 5 μsec. The ion source and RF fields remained on for another 30 μs for data acquisition. Only one wire or scraper was in the beam at a time; all other wires and scrapers were out of the beam-pipe aperture. The wire or scraper in the beam accumulated beam-induced charge over about 30 μsec. Only the charge collected over the last 10 μsec, when the beam was nearly in a steady state, was recorded and used to calculate the beam profiles. Then the injector was turned off, and the beam profile scanners were repositioned for the next cycle.

The rms emittances and the beam widths at different fractions of the peak intensity were among the quantities used to characterize the beam. The rms emittances at scanners 20 and 45 were calculated from a least-squares procedure using the rms measurements for the profiles at the four scanners in each cluster.

3 PRELIMINARY RESULTS FOR 75 mA

Measurements were made at 16, 50, 75, and 100 mA for a range of mismatch parameters, μ. In this paper we report only the preliminary results at 75 mA. The measured transverse profiles for the matched beams are Gaussian-like in the linear plots (not shown). Figures 2 and 3 show 75-mA matched and mismatched, respectively, beam profiles on a semilog scale at scanner 51. The matched rms beam size is 1.1 mm. Large amplitudes, up to 9 rms, are observed for the matched-beam case, much larger than would have been expected even for a mismatched beam, and indicating that a low-level halo is already present in the input beam. The incoming halo contributes a background at very low density, less than 10^{-3} to 10^{-4} of the peak intensity, as is seen in the plots. A better understanding of the source of this halo is required

The presence of this low-level background prevents us from using the maximum dynamic range to study the halo caused by mismatch. However, the beam widths at different intensity levels can be compared with the maximum predicted resonant-particle amplitude as a test of the Particle-Core Model, and these comparisons will be presented in a later publication.

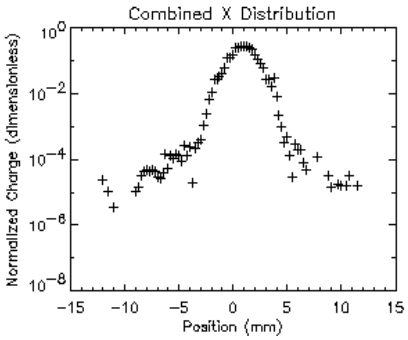

Figure 2: Matched (μ=1) horizontal beam profile at scanner 51 for 75 mA.

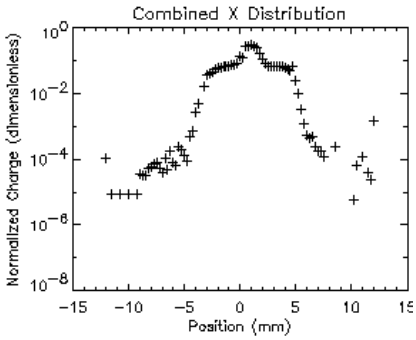

Figure 3: Mismatched (μ=1.5, breathing mode) horizontal beam profile at scanner 51 for 75 mA.

We have calculated the rms emittance growth from the measurements at the locations of scanners 20 and 45. The scanner 20 emittance-growth data were obtained from the rms beam sizes at scanners 20, 22, 24, and 26, and the scanner 45 emittance-growth data were obtained from scanners 45, 47, 49, and 51. Each of the rms emittances were obtained from a least-squares fit of calculated-to-measured rms beam sizes at the four scanners. TRACE3D was used to follow the rms beam envelope and to calculate the rms sizes at the four scanner locations. For both scanners 20 and 45, the Courant-Snyder transverse ellipse parameters in the x and y planes and the transverse emittances were adjusted to fit the eight measured rms sizes in x and y for four scanners. Figure 4 shows the transverse emittance (averaged over x and y) at scanners 20 and 45 for several mismatch parameters. Figure 5 shows the same plot for the emittances at the entrance and exit of the beam line from IMPACT code simulations [9]. As can be seen, our preliminary simulation results under-predict the measured emittance growth rates for mismatched beams. The simulations results shown use our best estimate of the RFQ output beam distribution from simulations as input to the beam line. The 6D input phase space distribution was not measured in the experiment. Additional simulations using different

possible input distributions show that input distributions with more extended tails generate more emittance growth. Detailed knowledge of the initial phase space distributions is required to obtain good agreement with the measured profiles.

After the measured emittances were obtained, space-charge tune depressions for an equivalent uniform beam were also calculated using TRACE3D. The tune depression is defined as the ratio of the phase advance per period σ, and the zero-current phase advance, σ_0. For a beam current of 75 mA, σ/σ_0=0.82 after the matching quadrupoles at scanner 4, and was constant at 0.95 after the beam had debunched by quadrupole 16. The effects of debunching in the transport line produce tune depressions that are weaker than those expected for comparable currents and energies in a proton linac (σ/σ_0~0.5 to 0.6).

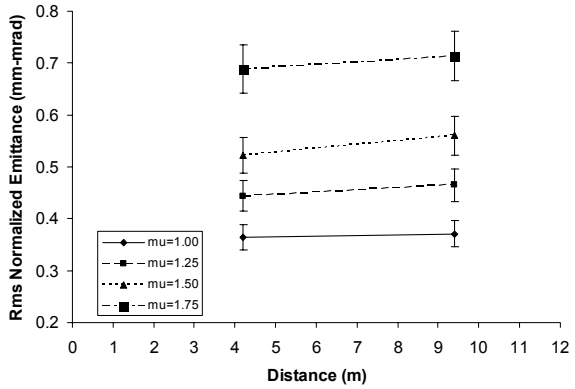

Figure 4: Average transverse rms emittance for several mismatches at scanners 20 and 45 for the breathing mode and a beam current of 75 mA.

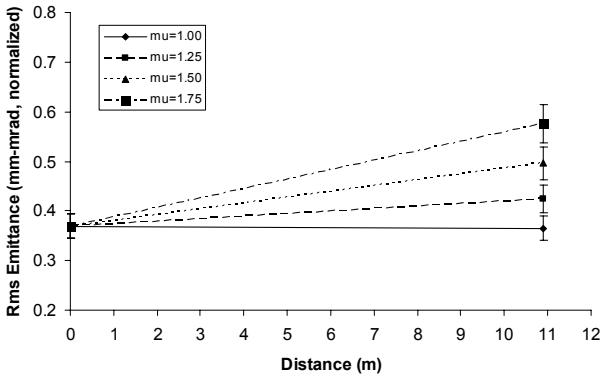

Figure 5: Simulation results for the average transverse rms emittance at the entrance and exit of the beam line for the breathing mode at 75 mA.

Preliminary results for the breathing-mode mismatches at 75 mA suggest a rapid rate of emittance growth that is consistent with a large fractional transfer of free energy to thermal energy within only a few mismatch oscillations (4 oscillations). Figure 6 shows the 75-mA rms emittance growth, averaged over x and y, at scanner 20 for the breathing mode as a function of μ. The theoretical predictions from the free-energy theory for the two calculated tune depressions are also shown in the figure and agree extremely well with the measured data.

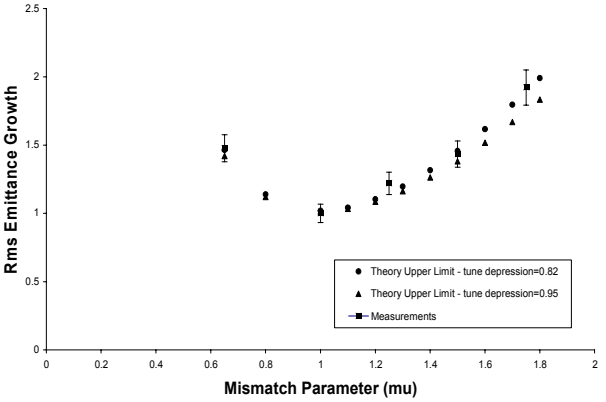

Figure 6: Rms-emittance growth, averaged over x and y, at scanner 20, 75mA, breathing mode.

4 REFERENCES

[1] J.S. O'Connell, T.P.Wangler, R.S.Mills, and K.R.Crandall, Proc. of 1993 Part. Accel. Conf., IEEE Catalog No. CH3279-7, 3657-3659.

[2] R.L. Gluckstern, Phys. Rev.Lett. 73, 1247 (1994).

[3] For an overview, see T.P.Wangler, K.R.Crandall, R.Ryne, and T.S.Wang, Phys.Rev. ST Accel. Beams 1 (084201)1998.

[4] P.L.Colestock, et.al, "Measurements of Halo Generation for a Proton Beam in a FODO Channel," Proc. 2001 Part. Accel. Conf., IEEE Catalog No. 01CH37268, 170-172.

[5] M. E. Schulze, et al, "Characterization of the Proton Beam from the 6.7 MeV LEDA RFQ," Proc. 2001 Part. Accel. Conf., IEEE Catalog No. 01CH37268, 591-593.

[6] T.P.Wangler, et al., Experimental Study of Proton-Beam Halo Induced by Beam Mismatch in LEDA," Proc. 2001 Part. Accel. Conf., IEEE Catalog No. 01CH37268, 2923-2925.

[7] J.D.Gilpatrick, et al., "Experience with the Low Energy Demonstration Accelerator (LEDA) Halo Experiment Beam Instrumentation," Proc. 2001 Part. Accel. Conf., IEEE Catalog No. 01CH37268, 2311-2313.

[8] J.D.Gilpatrick, et al., "Beam-Profile Instrumentation for Beam Halo Experiment: Overall Description and Operation," Proc. 2001 Part. Accel. Conf., IEEE Catalog No. 01CH37268, 525-527.

[9] J. Qiang, R. Ryne, S. Habib, and V. Decyk, "An Object-Oriented Particle-In-Cell Code for Beam Dynamics Simulation in Linear Acclerators, J. Comput. Phys. 163 (2000) 1.